Infrared phonons and specific heat in the gapped quantum magnet Ba3Cr2O8

Zhe Wang, M. Schmidt, A. Günther, Franz Mayr, Yuan Wan, S.-H. Lee, H. Ueda, Y. Ueda, Alois Loidl, Joachim Deisenhofer

Angaben zur Veröffentlichung / Publication details:

Wang, Zhe, M. Schmidt, A. Günther, Franz Mayr, Yuan Wan, S.-H. Lee, H. Ueda, Y. Ueda, Alois Loidl, and Joachim Deisenhofer. 2012. "Infrared phonons and specific heat in the gapped quantum magnet Ba3Cr2O8." *Physical Review B* 85 (22): 224304. https://doi.org/10.1103/physrevb.85.224304.

Infrared phonons and specific heat in the gapped quantum magnet $Ba_3Cr_2O_8$

Zhe Wang,[1] M. Schmidt,[1] A. Günther,[1] F. Mayr,[1] Yuan Wan,[2] S.-H. Lee,[3] H. Ueda,[4] Y. Ueda,[4] A. Loidl,[1] and J. Deisenhofer[1]

[1]*Experimental Physics V, Center for Electronic Correlations and Magnetism, Institute of Physics, University of Augsburg, D-86135 Augsburg, Germany*

[2]*Department of Physics and Astronomy, Johns Hopkins University, Baltimore, Maryland 21218, USA*

[3]*Department of Physics, University of Virginia, Charlottesville, Virginia 22904, USA*

[4]*Institute for Solid State Physics, University of Tokyo, Kashiwa 277-8581, Japan*

(Received 4 May 2012; revised manuscript received 15 June 2012; published 28 June 2012)

We report on the phonon spectrum of the spin-gapped quantum magnet $Ba_3Cr_2O_8$ determined by infrared spectroscopy, and on specific heat measurements across the Jahn-Teller transition in magnetic fields up to 9 T. Phonon modes split below the Jahn-Teller transition, which occurs at $T_{JT} = 70$ K as detected by specific-heat measurements. The field-dependent specific heat data is analyzed in terms of the contributions from lattice, magnetic and orbital degrees of freedom. In contrast to the isostructural compound $Sr_3Cr_2O_8$, our analysis does not indicate the existence of orbital fluctuations below the Jahn-Teller transition in $Ba_3Cr_2O_8$.

DOI: 10.1103/PhysRevB.85.224304 PACS number(s): 78.30.−j, 71.70.−d, 75.10.Hk

I. INTRODUCTION

Spin-gapped quantum antiferromagnets with dimerized ground states have been intensively studied due to the observation of various exotic phenomena in these systems.[1–4] Based on dimers of Cr^{5+} ($3d^1$, $S = 1/2$) or Mn^{5+} ($3d^2$, $S = 1$) ions, a series of isostructural dimerized compounds, such as $Ba_3Cr_2O_8$,[5–7] $Sr_3Cr_2O_8$,[8] and $Ba_3Mn_2O_8$[9] exhibits a magnon-condensation state with the application of an external magnetic field.[2]

The room-temperature crystalline structure of these compounds is hexagonal with space group $R\bar{3}m$.[5,10,11] In $Ba_3Cr_2O_8$ and $Sr_3Cr_2O_8$, a tetrahedral crystal field splits the $3d$ levels of the Cr ions into lower-lying doubly degenerated e orbitals and higher-lying triply degenerated t orbitals. Thus the systems are Jahn-Teller active, and they are expected to undergo a structural phase transition to remove the orbital degeneracy. Neutron powder diffraction indeed revealed such a structural transition at 70 K in $Ba_3Cr_2O_8$ and at 275 K in $Sr_3Cr_2O_8$ from hexagonal to monoclinic with space group $C2/c$.[5,11]

The magnetic susceptibility of $Ba_3Cr_2O_8$ has been reported by Nakajima *et al.*,[12] and Aczel *et al.*[13] They have shown that the susceptibility can be described by a Bleaney-Bowers model,[14] where they considered a magnetic structure consisting of weakly interacting spin dimers of Cr^{5+} ions. Fitting to this model resulted in an intradimer exchange interaction $J_0 = 2.15$ meV consistent with the value of 2.38 meV determined by neutron experiments.[5] The detailed magnetic structure has been studied theoretically based on extended Hückel tight-binding calculations.[15] The authors of Ref. 15 have examined all the possible exchange paths between the nearest-neighboring Cr ions. They found that the exchange interaction between adjacent Cr^{5+} ions in the hexagonal c_h direction is most important, while the other exchange interactions are much smaller. This was confirmed by inelastic neutron experiments in $Ba_3Cr_2O_8$.[5] The magnetic structure of $Sr_3Cr_2O_8$ is the same as $Ba_3Cr_2O_8$, but the intradimer exchange interaction of $Sr_3Cr_2O_8$ is 5.55 meV,[16] about twice the corresponding value in $Ba_3Cr_2O_8$, and the Jahn-Teller transition temperature 285 K in $Sr_3Cr_2O_8$ is about four times higher than that in $Ba_3Cr_2O_8$.[17] In addition, an anomalous strong damping of the optical phonon modes has been observed down to about 120 K in $Sr_3Cr_2O_8$, which is below the Jahn-Teller transition temperature of $Sr_3Cr_2O_8$.[17,18] Moreover, an analysis of the specific heat revealed a residual orbital entropy below the structural transition, indicating strong fluctuations in the orbital degrees of freedom.

In this work, we investigated the polar phonons and the specific heat in $Ba_3Cr_2O_8$ to search for a similar fluctuation regime. We have resolved the phonon spectra from the reflectivity measurements and found the splitting of phonon modes right below the Jahn-Teller transition, indicating that strong fluctuations of the lattice degrees of freedom are absent in $Ba_3Cr_2O_8$. This clearly distinguishes the system from $Sr_3Cr_2O_8$. The analysis of the specific heat confirms this difference between the compounds, because the orbital entropy associated with the splitting of the orbital ground state is completely recovered at the Jahn-Teller transition in $Ba_3Cr_2O_8$.

II. EXPERIMENTAL DETAILS

Single crystals of $Ba_3Cr_2O_8$ were grown by the floating-zone method. They were cleaved perpendicular to the hexagonal c_h axis and checked by single-crystal x-ray diffraction. The heat capacity was measured in a Quantum Design physical properties measurement system at temperatures $1.8 < T < 300$ K with applied magnetic fields up to 9 T. Reflectivity measurements were carried out on optically polished samples for $4 < T < 300$ K in the far- and mid-infrared range using the Bruker Fourier-transform infrared spectrometers IFS 113v and IFS 66v/S with a He-flow cryostat (Cryovac).

III. EXPERIMENTAL RESULTS AND DISCUSSION

A. Infrared spectra

Figure 1 shows reflectivity spectra of $Ba_3Cr_2O_8$ measured for the radiation electric field **E** parallel with the crystalline hexagonal a_hb_h-plane (**E** $\parallel$ a_hb_h plane) at 295 and 4 K, which are above and below the Jahn-Teller transition temperature $T_{JT} = 70$ K, respectively. The seven modes observed above T_{JT}

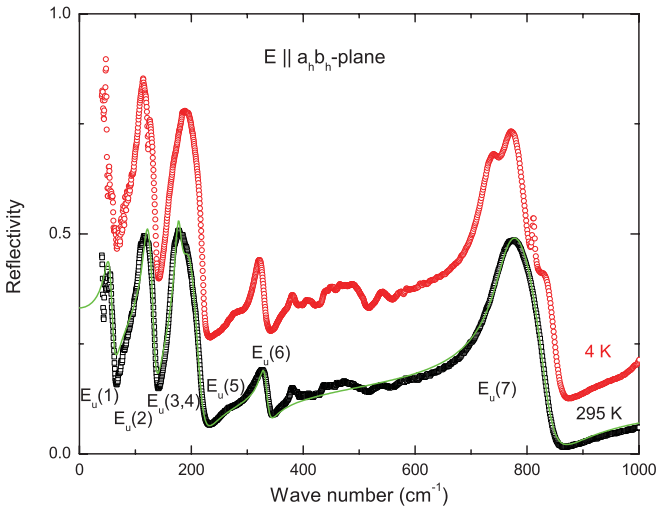

FIG. 1. (Color online) Reflectivity spectra of $Ba_3Cr_2O_8$ measured with $\mathbf{E} \parallel a_h b_h$ plane at 295 and 4 K. The spectrum of 4 K is shifted with respect to that of 295 K by a constant of 0.1. Infrared-active phonon mode $E_u(j)(j = 1,\ldots,7)$ are marked at the spectrum of 295 K for the hexagonal structure. Solid line is a fit of Drude-Lorentz model to the data of 295 K as described in the text.

are tentatively assigned as $E_u(j)$ $(j = 1,...,7)$. The primitive unit cell of the high-temperature hexagonal structure with space group $R\bar{3}m$ (No. 166)[19,20] contains one chemical formula unit and, hence, a total of 39 normal modes exist. The IR active modes are characterized by the irreducible representations $6A_{2u}(\mathbf{E} \parallel c_h) + 7E_u[\mathbf{E} \parallel (a_h,b_h)]$.[5,21] The number of normal modes is in agreement with the observation of infrared and Raman active phonons reported for the isostructural system $Sr_3Cr_2O_8$.[17,18] The overall appearance of the $Ba_3Cr_2O_8$ far-infrared spectra for $\mathbf{E}\|(a_h,b_h)$ are similar to the ones of $Sr_3Cr_2O_8$, but the $Ba_3Cr_2O_8$ phonons are shifted to lower eigenfrequencies consistent with the larger molar mass of $Ba_3Cr_2O_8$.[17] The absolute value of the reflectivity is relatively low, which might be due to the imperfection of the sample surface, and similar values have been found for $Sr_3Cr_2O_8$.[17] The weak features in the frequency range between modes $E_u(6)$ and $E_u(7)$ are also assigned to originate from defects on the sample's surface.

The quantitative analysis of the phonon modes is performed by fitting the reflectivity spectrum with the Drude-Lorentz model. According to this model, the phonon contribution of the complex dielectric function is given by

$$\epsilon(\omega) = \epsilon_\infty + \sum_j \frac{\Omega_j^2}{\omega_{0j}^2 - \omega^2 - i\gamma_j\omega}, \qquad (1)$$

where each phonon mode j is described by the eigenfrequency ω_{0j}, damping coefficient γ_j and effective ionic plasma frequency Ω_j. The parameter ϵ_∞ takes into account contributions of higher-lying electronic excitations and was used as a free fitting parameter ranging between ~4 at room temperature and ~7 just above the Jahn-Teller transition. At normal incidence, the reflectivity $R(\omega)$ is related to $\epsilon(\omega)$ via

$$R(\omega) = \left|\frac{\sqrt{\epsilon(\omega)} - 1}{\sqrt{\epsilon(\omega)} + 1}\right|^2. \qquad (2)$$

TABLE I. Eigenfrequency ω_0, effective ionic plasma frequency Ω and damping coefficient γ of all $7E_u$ phonon modes in $Ba_3Cr_2O_8$ at 295 K.

E_u	7 Phonons		
Mode	ω_0 (cm^{-1})	Ω (cm^{-1})	γ(cm^{-1})
1	52.6	101.2	13.5
2	119.7	187.9	14.0
3	174.7	182.8	10.6
4	188.4	174.1	26.2
5	274.7	166.0	172.1
6	330.5	120.4	14.9
7	759.2	718.2	45.5

The fit result for the room-temperature spectrum using seven oscillators is given by the solid line in Fig. 1, which agrees well with the experimental data. Note that the lowest lying mode $E_u(1)$ could not be completely resolved and only the high frequency flank has been fitted. Thus, the fitting parameters for $E_u(1)$ contain a larger experimental uncertainty. The fitting parameters for the $7E_u$ modes are listed in Table I.

For the monoclinic $C2/c$ (No. 15b) structure below the JT transition, the number of expected normal IR modes increases to $19A_u$ for the radiation electric field parallel with monoclinic b_m axis and $20B_u$ for the electric field parallel with monoclinic $a_m c_m$-plane, i.e., $\Gamma = 19A_u(\mathbf{E} \parallel b_m) + 20B_u[\mathbf{E} \parallel (a_m,c_m)]$.[5,21] According to the geometric relation between hexagonal and monoclinic axes $a_h = \frac{1}{2}(a_m - b_m)$, $b_h = -\frac{1}{2}(a_m + b_m)$, and $c_h = \frac{3}{2}c_m - \frac{1}{2}a_m$ determined by neutron diffraction measurements,[11,16] the IR spectra measured with $\mathbf{E} \parallel a_h b_h$ plane below T_{JT} should display all the $19A_u$ and $20B_u$ modes. However, the coexistence of three monoclinic twins in the single crystal[5,16] and the low monoclinic symmetry make it difficult to determine the eigenfrequency, damping coefficient and plasma frequency of the phonon modes below the Jahn-Teller transition.[22]

The temperature-dependent reflectivity spectra reveal that the hexagonal mode of $E_u(2)$ and $E_u(7)$ split below T_{JT}, while a splitting of the other modes, which are hardening with decreasing temperature, could not be resolved below T_{JT}. Therefore we focus on the temperature-dependent features of modes $E_u(2)$ and $E_u(7)$, and try to describe the low-temperature modes with Lorentzian functions according to Eqs. (1) and (2). As indicated by the arrows in Fig. 2, we model the low-temperature spectra with two oscillators for both the $E_u(2)$ and the $E_u(7)$ modes. For the monoclinic structure, the phonon modes cannot be uniquely determined in a single polarization measurement. Therefore the obtained fit parameters including ϵ_∞ do not necessarily reflect the intrinsic dielectric properties of the system and it might be misleading to show the dielectric parameters. Instead, the reflectivity spectra should be measured with three different polarizations so as to determine the three independent matrix elements of the dielectric matrix for $\mathbf{E} \parallel a_m c_m$ plane.[22] This is infeasible for $Ba_3Cr_2O_8$ with the coexistencce of three monoclinic twins.[5,16] Thus the modeling here with Lorentzian functions is rather a way to parametrize the reflectivity spectra and reveal clear changes occurring at T_{JT}.

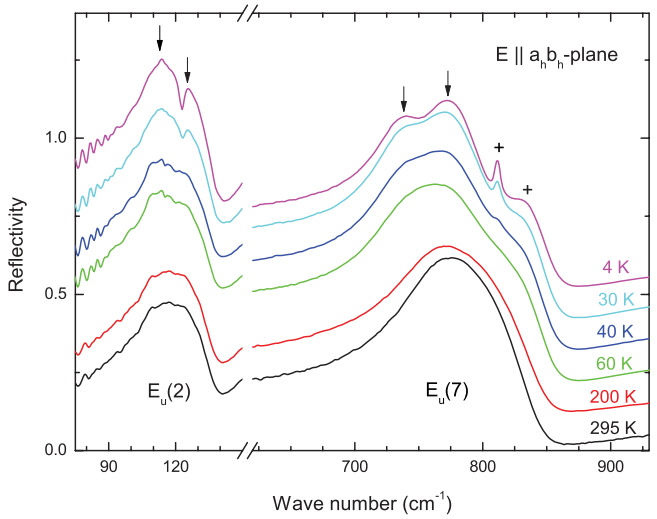

FIG. 2. (Color online) Reflectivity spectra corresponding to IR phonon modes $E_u(2)$ and $E_u(7)$ measured with $\mathbf{E} \parallel a_h b_h$ plane at various temperatures. The spectra are shifted with respect to that at 295 K by a constant in order to clearly illustrate the evolution of phonon modes with decreasing temperature.

The fitting results of eigenfrequency, damping coefficient and plasma frequency are summarized as a function of temperature in Fig. 3, which clearly shows the splitting of phonons right below T_{JT}, consistent with the phase transition to monoclinic structure. This is an evident contrast to the case of $Sr_3Cr_2O_8$, which is an isostructural compound of $Ba_3Cr_2O_8$.[11] In $Sr_3Cr_2O_8$, the new phonons are not emerging right below the Jahn-Teller transition due to strong fluctuations. With decreasing temperature, the fluctuations are reduced and all

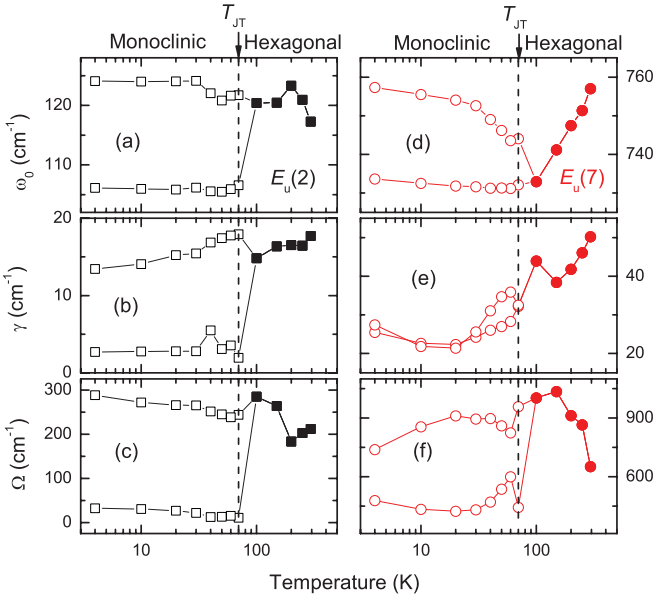

FIG. 3. (Color online) Temperature dependence of eigenfrequency (a) and (d), damping coefficient (b) and (e) and ionic plasma frequency (c) and (f) for modes $E_u(2)$ and $E_u(7)$ on a semilogarithmic scale. The Jahn-Teller transition temperature T_{JT} is indicated by vertical dashed line. Open symbols signify the results of parametrization below T_{JT} (see text).

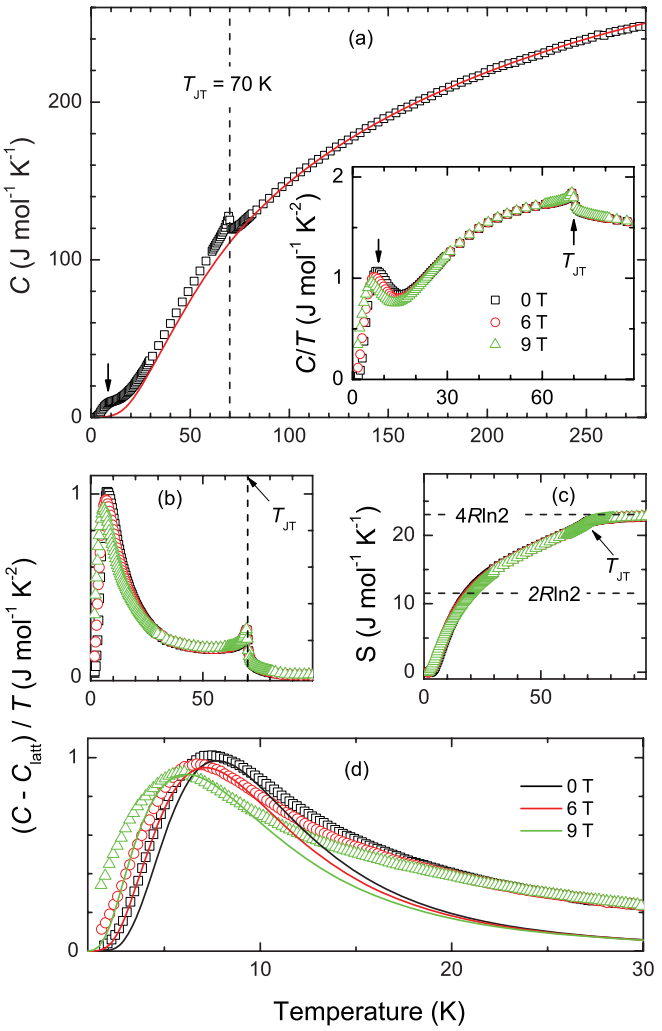

FIG. 4. (Color online) (a) Specific heat of $Ba_3Cr_2O_8$ without applied magnetic field. Solid line is a fit of lattice contribution to specific heat according to Debye and Einstein models as described in the text. Inset shows specific heat divided by temperature C/T measured at various magnetic fields. (b) Residual specific heat $(C - C_{latt})/T$ and (c) the corresponding entropy obtained at different fields. (d) Magnetic contribution to specific heat fitted by considering the Zeeman interaction of isolated spin dimers with magnetic field (solid lines) as described in the text.

the modes of monoclinic structure are observed when the temperature is lower than 100 K.[17]

The modes marked by "+" in Fig. 2 at 812 and 834 cm^{-1} are visible right at 40 K and lower temperatures. These modes could be new phonon modes of the monoclinic structure, which have small spectral weight and large damping effect that could not be distinguished from the strong modes corresponding to $E_u(7)$ at higher temperatures.

B. Specific heat

Figure 4(a) shows the specific heat of $Ba_3Cr_2O_8$ measured as a function of temperature. Two anomalies can be observed in the specific-heat data. A sharp anomaly indicated by a dashed vertical line can be easily recognized at 70 K. Another feature observed below 20 K is marked by an arrow. The inset of

Fig. 4(a) shows the specific heat over temperature C/T vs T measured in various external magnetic fields. The anomaly at $T_{JT} = 70$ K is independent on the magnitude of magnetic field, and marks the structural phase transition from hexagonal $R\bar{3}m$ to monoclinic $C2/c$, in agreement with the results obtained from neutron diffraction measurements.[5] The anomaly below 20 K is very sensitive to the magnitude of the magnetic field indicating that it is related to the spin degrees of freedom.

The lattice contribution to the specific heat C_{latt} can be described according to the phononic spectra that have been determined in Sec. III A. We model the lattice contribution by a sum of one isotropic Debye (D) and four isotropic Einstein terms ($E_{1,2,3,4}$) with the fixed ratio $D : E_1 : E_2 : E_3 : E_4 = 1 : 3 : 4 : 3 : 2$ between these terms accounting for the 39 degrees of freedom per formula unit. This ratio has been previously used to describe the specific-heat data of $Sr_3Cr_2O_8$.[17] The resulting contribution to the specific heat shown as a solid line in Fig. 4(a) has been obtained with the Debye and Einstein temperatures $\theta_D = 123$ K, $\theta_{E1} = 137$ K, $\theta_{E2} = 265$ K, $\theta_{E3} = 658$ K, and $\theta_{E4} = 1270$ K in agreement with the frequency ranges where IR active phonons of the hexagonal structure occur. The fitting curve agrees well with the specific-heat data above T_{JT}, while below T_{JT} it deviates from the experimental data indicating that the magnetic and orbital contributions to the specific heat are important below the Jahn-Teller transition. Since $Ba_3Cr_2O_8$ has larger molecular mass than $Sr_3Cr_2O_8$, the obtained Debye and Einstein temperatures of $Ba_3Cr_2O_8$ should be lower than those of $Sr_3Cr_2O_8$.[17] The fitted Debye-temperature ratio between $Ba_3Cr_2O_8$ and $Sr_3Cr_2O_8$is 0.91, which is consistent with the ratio $\sqrt{m_{\text{SCO}}} : \sqrt{m_{\text{BCO}}} = 0.88$, where m_{SCO} and m_{BCO} are the molecular masses of $Sr_3Cr_2O_8$and $Ba_3Cr_2O_8$, respectively.

The residual specific heat divided by temperature $(C - C_{\text{latt}})/T$ is shown in Fig. 4(b). One can clearly recognize a λ-shaped anomaly at the Jahn-Teller transition around 70 K and the magnetic anomaly below 20 K, which are well separated in the temperature scale. The corresponding entropy $S(T) = \int_0^T d\vartheta (C - C_{\text{latt}})/\vartheta$ reaches a value slightly lower than the expected $S = 4R \ln 2$ for the sum of magnetic and orbital contribution as shown in Fig. 4(c), where R is the molar gas constant. For a spin-1/2 dimer, the entropy increases by $2 \ln 2$ from the ordered to the disordered spin state. Because there is essentially one spin dimer per formula unit of $Ba_3Cr_2O_8$, the magnetic contribution to the entropy should be $2R \ln 2$. This is reached at 20 K indicated in Fig. 4(c). At this temperature, the specific heat measured at different fields begins to deviate from each other on cooling. Above the Jahn-Teller transition the e orbitals of each Cr^{5+} ion are degenerate and the orbital degrees of freedom will contribute to the entropy by another $2R \ln 2$, where the two Cr ions per formula unit have been taken into account.

In order to describe the magnetic contribution to the specific heat, we consider a model with the intradimer exchange interaction and the Zeeman interaction but ignore the inter-dimer exchange interactions, which are much smaller than the intradimer interaction.[5] Thus we can model the magnetic contribution to the specific heat by $C_{\text{mag}}(T) = N \frac{\partial E}{\partial T}$ using $E = \frac{1}{Z} \sum_{i=0}^{3} \epsilon_i e^{-\beta \epsilon_i}$ with the partition function $Z = \sum_{i=0}^{3} e^{-\beta \epsilon_i}$ and the energies $\epsilon_{0,1,2,3} = 0, J_0 - g\mu_B H, J_0, J_0 + g\mu_B H$, where μ_B is the Bohr magneton, H is the magnetic field, and $\beta \equiv 1/k_B T$ with the Boltzmann constant k_B. The solid lines in Fig. 4(d) are the calculated specific heat curves according to this model, where the intradimer exchange interaction $J_0 = 2.38$ meV was determined by inelastic neutron experiments,[5] and the g factor $g = 1.94$ was measured by electron spin resonance experiments.[5] This simple model captures the most important features of the experimental data. The modeled specific heat reaches the maximum nearly at the same temperature as that of the experimental data. The maximum shifts to lower temperature and becomes smaller with the increase of magnetic field, since the gap between the lower-lying triplet state and the singlet state is reduced due to Zeeman interaction with the magnetic field. Because interdimer interactions are not considered in the model, the modeled specific heat should be smaller than the experimental data as observed in Fig. 4(d). Note that this discrepancy could also originate to a certain amount from the uncertainties of the changes in the phonon density of states in the low-temperature structure.

IV. CONCLUSION

In summary, the infrared phonon spectrum measured with the polarization perpendicular to the hexagonal c_h axis in $Ba_3Cr_2O_8$ exhibits all expected 7 E_u modes above the structural phase transition at 70 K. Below this transition, which is associated with a Jahn-Teller distortion and orbital ordering, a splitting of some phonon modes and the appearance of new modes indicate the reduced symmetry in the distorted phase. In the specific heat a clear anomaly is visible at 70 K, which does not change with applied magnetic field. An additional low-temperature anomaly in the specific heat is assigned to originate from magnetic excitations and its dependence on magnetic field can be explained by considering the thermal population of triplet states and their Zeeman splitting in external magnetic fields. The entropy change associated with orbital ordering is found to be reached just above the structural Jahn-Teller transition without any sign of orbital fluctuations below 70 K. In comparison with the isostructural compound $Sr_3Cr_2O_8$, where the polar phonons and the specific heat bear signatures of strong fluctuations and competing interactions, the fact that this is not the case for $Ba_3Cr_2O_8$ might help to understand which interactions are responsible for the curious behavior of $Sr_3Cr_2O_8$ and single out the differences in these otherwise very similar systems.

ACKNOWLEDGMENTS

We want to thank V. Tsurkan and D. Vieweg for experimental support. This work is supported by the Deutsche Forschungsgemeinschaft (DFG) partially within the Transregional Collaborative Research Center TRR 80 (Augsburg-Munich) and the Research Unit FOR 960. ZW and MS acknowledge the support from UA through the TRR80 graduate school. Work at UVa was supported by the US Department of Energy, Office of Basic Energy Sciences, Division of Materials Sciences and Engineering under Award DE-FG02-10ER46384.

[1]P. Lemmens, G. Guntherodt, and C. Gros, Phys. Rep. **375**, 1 (2003).
[2]T. Giamarchi, C. Rüegg, and O. Tchernyshyov, Nat. Phys. **4**, 198 (2008).
[3]D. V. Zakharov, J. Deisenhofer, H.-A. Krugvon Nidda, P. Lunkenheimer, J. Hemberger, M. Hoinkis, M. Klemm, M. Sing, R. Claessen, M. V. Eremin, S. Horn, and A. Loidl, Phys. Rev. B **73**, 094452 (2006).
[4]Z. Wang, M. Schmidt, Y. Goncharov, Y. Skourski, J. Wosnitza, H. Berger, H.-A. Krug von Nidda, A. Loidl, and J. Deisenhofer, J. Phys. Soc. Jpn. **80**, 124707 (2011); R. M. Eremina, T. P. Gavrilova, A. Günther, Z. Wang, M. Johnsson, H. Berger, H.-A. Krug von Nidda, J. Deisenhofer, and A. Loidl, Eur. Phys. J. B **84**, 391 (2011); J. Deisenhofer, R. M. Eremina, A. Pimenov, T. Gavrilova, H. Berger, M. Johnsson, P. Lemmens, H.-A. Krug von Nidda, A. Loidl, K.-S. Lee, and M.-H. Whangbo, Phys. Rev. B **74**, 174421 (2006).
[5]M. Kofu, J.-H. Kim, S. Ji, S.-H. Lee, H. Ueda, Y. Qiu, H.-J. Kang, M. A. Green, and Y. Ueda, Phys. Rev. Lett. **102**, 037206 (2009).
[6]T. Dodds, B.-J. Yang, and Y. B. Kim, Phys. Rev. B **81**, 054412 (2010).
[7]A. A. Aczel, Y. Kohama, M. Jaime, K. Ninios, H. B. Chan, L. Balicas, H. A. Dabkowska, and G. M. Luke, Phys. Rev. B **79**, 100409 (2009).
[8]A. A. Aczel, Y. Kohama, C. Marcenat, F. Weickert, M. Jaime, O. E. Ayala-Valenzuela, R. D. McDonald, S. D. Selesnic, H. A. Dabkowska, and G. M. Luke, Phys. Rev. Lett. **103**, 207203 (2009).
[9]E. C. Samulon, Y. Kohama, R. D. McDonald, M. C. Shapiro, K. A. Al-Hassanieh, C. D. Batista, M. Jaime, and I. R. Fisher, Phys. Rev. Lett. **103**, 047202 (2009).
[10]M. B. Stone, M. D. Lumsden, Y. Qiu, E. C. Samulon, C. D. Batista, and I. R. Fisher, Phys. Rev. B **77**, 134406 (2008).
[11]L. C. Chapon, C. Stock, P. G. Radaelli, and C. Martin, arXiv:0807.0877v2.
[12]T. Nakajima, H. Mitamura, and Y. Ueda, J. Phys. Soc. Jpn. **75**, 054706 (2006).
[13]A. A. Aczel, H. A. Dabkowska, P. R. Provencher, and G. M. Luke, J. Cryst. Growth **310**, 870 (2008).
[14]B. Bleaney and K. D. Bowers, Proc. Roy. Soc. A (London) **214**, 451 (1952).
[15]H. J. Koo, K. S. Lee, and M. H. Whangbo, Inorg. Chem. **45**, 10743 (2006).
[16]D. L. Quintero-Castro, B. Lake, E. M. Wheeler, A. T. M. N. Islam, T. Guidi, K. C. Rule, Z. Izaola, M. Russina, K. Kiefer, Y. Skourski, and T. Herrmannsdorfer, Phys. Rev. B **81**, 014415 (2010).
[17]Zhe Wang, M. Schmidt, A. Günther, S. Schaile, N. Pascher, F. Mayr, Y. Goncharov, D. L. Quintero-Castro, A. T. M. N. Islam, B. Lake, H.-A. Krug von Nidda, A. Loidl, and J. Deisenhofer, Phys. Rev. B **83**, 201102 (2011).
[18]D. Wulferding, P. Lemmens, K.-Y. Choi, V. Gnezdilov, Y. G. Pashkevich, J. Deisenhofer, D. Quintero-Castro, A. T. M. NazmulIslam, and B. Lake, Phys. Rev. B **84**, 064419 (2011).
[19]H. J. Mattausch and H. K. Muller-Buschbaum, Z. Naturforsch. B **27**, 739 (1972); A. A. Aczel, H. A. Dabkowska, J. F. Britten, L. E. Harrington, and G. M. Luke, Acta Cryst. E **63**, i196 (2007).
[20]H. Arnold, in *International Tables for Crystallography*, edited by T. Hahn, (Kluwer Academic, Dordrecht, 1989), Vol. A, Chap. 5.
[21]E. Kroumova, M. I. Aroyo, J. M. Perez-Mato, A. Kirov, C. Capillas, S. Ivantchev, and H. Wondratschek, Phase Transitions **76**, 155 (2003).
[22]A. B. Kuz'menko, E. A. Tishchenko, and V. G. Orlov, J. Phys.: Condens. Matter **8**, 6199 (1996).